

Deep Level Defects in He-implanted n-6H-SiC Studied by Deep Level Transient Spectroscopy

X. D. Chen, C. C. Ling,* S. Fung, C. D. Beling, and H. S. Wu

Department of Physics, The University of Hong Kong, Pokfulam Road, Hong Kong, P. R. China

G. Brauer, W. Anwand, and W. Skorupa

Institut für Ionenstrahlphysik und Materialforschung, Forschungszentrum Rossendorf, Postfach 510119, D-01314 Dresden, Germany

ABSTRACT

Deep level transient spectroscopy (DLTS) was used to study deep level defects in He-implanted n-type 6H-SiC samples. Low dose He-implantation (fluence $\sim 2 \times 10^{11}$ ions/cm²) has been employed to keep the as-implanted sample conductive so that studying the introduction and the thermal evolution of the defects becomes feasible. A strong broad DLTS peak at 275K-375K (called signal B) and another deep level at $E_C-0.50\text{eV}$ were observed in the as-implanted sample. The intensity of the peak B was observed to linearly proportional to the logarithm of the filling pulse width, which is a signature for electron capture into a defect related to dislocation. After annealing at 500°C, the intensity of peak was significantly reduced and the remained signal has properties identical to the well known Z_1/Z_2 deep defects, although it is uncertain whether the Z_1/Z_2 exist in the as-implanted sample or it is the annealing product of the dislocation-related defect. The E_1/E_2 defect ($E_C-0.3/0.4\text{eV}$) was not presence in the as-implanted sample, but was observed after the 300°C annealing.

INTRODUCTION

Silicon carbide (SiC) is a wide band-gap semiconductor material having unique physical and electronic properties for fabricating high-temperature, high-power, and high-frequency electronic devices [1]. Ion-implantation is an important technique for the selective doping of SiC because of the extremely small diffusion constants of the dopant impurities in SiC. Defects are usually induced by the ion implantation or the post-implantation annealing processes and some of these defects do not anneal out at very high temperatures [2-4]. Ion implantation or particle irradiation induced deep level defects in SiC have been extensively studied by capacitance transient techniques such as deep level transient spectroscopy (DLTS) [2-11]. Deep levels at $E_C-0.6/0.7\text{eV}$ (termed Z_1/Z_2) are generated either by electron irradiation or by ion implantation, and the concentration of these centers is reduced by annealing below 1000°C. Another pair of important deep levels $E_C-0.3/0.4\text{eV}$ are usually referred to E_1/E_2 and the concentration of these centers is strongly reduced (the DLTS signal of E_1/E_2 is below the detection limit) by annealing at 1200-1400°C [2-11]. E_1/E_2 are the dominant peaks in the DLTS spectra of the as-electron-irradiated 6H-SiC samples [4-8]. For the cases of deuterium implanted [4], He implanted [3,6,9], and neutron irradiated [10] n-type 6H-SiC, E_1/E_2 are not the peaks having the highest intensities. However their intensities increase with increasing annealing temperature before they start annealing out [3,4,10]. The less prominent peaks labeled E_i at $\sim E_C-0.50\text{eV}$ is usually observed in electron

irradiated n-type 6H-SiC materials and they anneal out at a relatively low temperature of $\sim 300^{\circ}\text{C}$ [7]. RD5 is another defect observed in He-implanted 6H-SiC and it has an ionization energy of 0.43-0.47eV.

In this work, n-type 6H-SiC samples were implanted with He ion with a relatively low dosage (fluence $\sim 2 \times 10^{11}$ ions/cm²) so that the as-implanted samples remained in the conductivity range suitable for DLTS measurement. DLTS technique was then employed to study the formation and the thermal evolution of the deep level defects induced by the He implantation process

EXPERIMENTAL DETAILS

The starting n-type 6H-SiC material used in the present study was 5- μm -thick nitrogen doped (0001) oriented epitaxial layer (1×10^{16} cm⁻³) grown on n⁺-type 6H-SiC substrate (8×10^{17} cm⁻³) purchased from Cree Research Inc. The samples were rinsed in boiling acetone, ethanol, and de-ionized water, and were then chemically treated in 10% hydrofluoric acid solution to remove the oxidation layer. Large area Ohmic contacts were made by evaporating Al on the substrate backside of the samples followed by a 5 min annealing process at 900°C in pure nitrogen gas.

The samples were implanted with He ions at energies of 55keV, 210keV, 430keV, 665keV and 840keV (each with fluence of $\sim 2 \times 10^{11}$ ions/cm²) so as to produce a 2 μm deep box-shape implanted layer. Schottky contacts for DLTS measurement were prepared by thermally evaporating gold dots of 0.6 mm diameter on the implanted surface of the epitaxial layer. The quality of all the Schottky-diode-like samples was monitored by observing the current-voltage (I-V) and the capacitance-voltage (C-V) characteristics. Each of the isochronal thermal annealing steps was carried out in the argon atmosphere for 30 min.

DLTS spectra were taken in the temperature range of 100-400K. The ionization energies and the capture cross sections of the deep level defects were determined from the Arrhenius plots. The trap concentrations were evaluated from the peak heights of the DLTS signal. In the calculations, the defect capture cross sections were assumed to be temperature independent.

RESULTS AND DISCUSSION

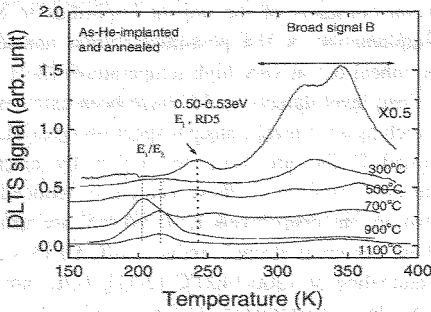


Figure 1. DLTS spectra for He-implanted n-type 6H-SiC with subsequent annealing at 300°C , 500°C , 700°C , 900°C , and 1100°C , respectively.

Figure 1 shows the DLTS spectra of the He-implanted samples subjected to different annealing conditions. DLTS measurements were also performed on the as-grown control sample and no deep level signal was observed (detection limit $\sim 10^{13} \text{ cm}^{-3}$). This indicates that all the observed defect levels are induced by the He implantation. For the as-He-implanted sample, peak at $\sim 240\text{K}$ and a broad signal (denoted by B) were clearly observed. From the Arrhenius plots in figure 2, the activation energies of the 240K peak and the broad peak B was $E_C-0.50\text{eV}$ and $E_C-0.89\text{eV}$ respectively.

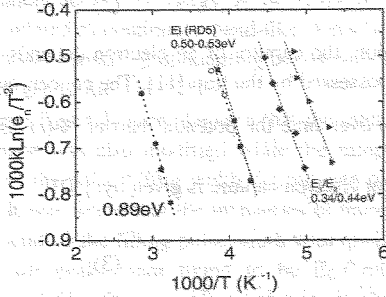


Figure 2. Arrhenius plots of the emission rates $1000kLn(e_n/T^2)$ vs reciprocal temperature for the observed deep level defects, respectively.

In order to investigate the nature of the broad signal in the as-implanted sample, DLTS spectra with different filling pulse width and different reverse bias voltage were taken and they were shown in figure 3.

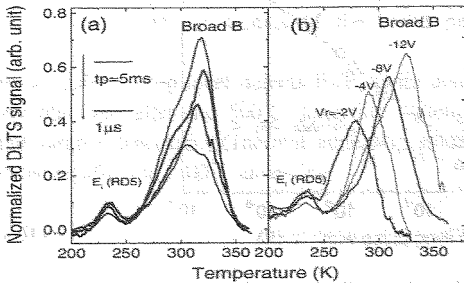


Figure 3. DLTS spectra obtained under (a) different filling pulse duration time t_p ; and (b) reverse bias V_r for the as-He-implanted n-type 6H-SiC.

For the spectra with different filling pulse width t_p , it can be clearly seen that the broad peak B consists of more than one peak and these peaks' intensities have different filling pulse width dependence. Interestingly, the intensities of the observed dominant peak (the broad peak B) increase even with filling pulse widths longer than 10 ms (as shown in Fig.3(a)) and the peak temperature position are found to shift to higher temperature using the same rate window with varying of measurement reverse bias (as shown in Fig3 (b)).

For ideal point defects, electron capture of the trap is described by the rate equation:

$$\frac{dN_f}{dt} = -nv\sigma_n(N_{total} - N_f) \quad (1)$$

N_f is the filled electron trap density, N_{total} is the total trap density, n is the free electron density, v is the free electron thermal velocity and σ_n is the capture cross section of the trap. This implies after the filling pulse period of t_p , the filled electron trap density would be equal to:

$$N_f(t_p) = N_T(1 - \exp[-nv\sigma_n t_p]) \quad (2)$$

However, for a defect related to the dislocation, the capture of an electron depends on the potential barrier and thus the charge already possessed by the trap [11]. The concentration of the free electrons that have enough energy to overcome the potential barrier $\Phi(t)$ is given

by: $n \exp(-q\Phi(t)/kT)$. The rate equation for electron capture is given by: [12]

$$\frac{dN_f}{dt} = \sigma_n v n N_T [1 - f(t)] \exp\left(-\frac{q\Phi(t)}{kT}\right), \quad (3)$$

$f(t)$ is the fraction of traps being filled and thus $N_f = f N_T$. The time evolution of electron capture of the dislocation is given by: [12]

$$N_f(t_p) = \sigma_n v n n N_T \ln[(t_p + \tau)/\tau], \quad (4)$$

where τ is a constant.

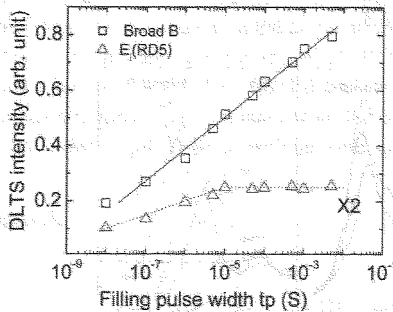


Figure 4 Dependence of the observed peak amplitudes on the logarithm of filling pulse time t_p ranging from 0.1 μ s to 10ms in the as-He-implanted sample.

Figure 4 shows the DLTS intensities of the broad signal B and the 0.50eV peak as a function of t_p . The data of the broad peak B follow a linear relationship for over four orders of magnitude of t_p and the increase of the intensity of the signal B with $\log(t_p)$ over a wide range from 10^{-8} s to 10^{-2} s, moreover, the peak intensity of peak B increases with increasing filling pulse width even for filling pulse width as large as 10ms indicating that the broad peak B is indeed related to defects due to dislocation-like or point-defect cluster with dangling bonds, where charge buildup potential barrier governs the capture rate (refer to equation (4)).

The saturation of the 0.50eV peak intensity at large t_p is the typical behavior for point defect, as from equation (2) $N_f(t_p)$ saturates as $t_p \gg (n\nu\sigma_n)^{-1}$. On the other hand, DLTS measurements under different reverse bias show the bias dependence of the deep level activation energies (as shown in figure 3(b)). The Arrhenius plot in figure 2 shows that the activation energies of signal B is $E_C-0.89$ eV. It was found that with reverse bias $V_r = -1$ V, the activation energy for signal B has changed to $E_C-0.6$ eV. For the case of the 0.5eV signal, the deduced activation energy does not show any noticeable change with respect to the bias voltage. The reverse bias dependent activation energy of the of the broad peak B indicate that the broad peak B should be related to continuous band-like states, which was expected of the model involving a defect cluster consisting of dangling bonds, which introduce the continuous band-like states in the band gap of SiC [11,12].

From figure 1, it can be seen that the intensity of signal B was significantly reduced and its shape was also modified while the sample anneals up to 500 °C. We have also investigated the pulse filling width dependence of this broad signal for the 500°C annealed sample. It was found that the intensities of these two peaks in the 500°C annealed sample do not depend on the filling pulse width with $t_p > 100\mu s$. Moreover, the activation energies of these two peaks were found to be $E_C-0.6/0.7$ eV, which are close to those of the well-known Z_1/Z_2 . This annealing behavior is also similar to that of the deep level Z_1/Z_2 . We thus suggest that the peaks observed at $T=300-350$ K in the DLTS spectra of samples annealed at 500°C or above be the Z_1/Z_2 deep levels. This implies that the dislocation related defect contained in the broad signal has already been annealed out at 500°C. As seen from the DLTS spectrum of the as-implanted sample in figure 1, it has already been pointed out that the broad signal should consist of more than one signal and the intensity dependences of these signals have different filling pulse width dependence. We thus conclude that the Z_1/Z_2 also exists in the as-implanted sample although it is difficult to unambiguously decompose the signals of the broad peak in the as-implanted sample spectrum.

Another pair of deep level defects E_1/E_2 (with activation energies of $E_C-0.3/0.4$ eV) were clearly observed after the 500°C annealing although they were not present in the as-implanted sample spectrum. Thermal annealing studies showed that these two peaks were still detected after the 1100°C annealing.

CONCLUSION

Low dose He-implantation induced deep level defects in n-6H-SiC were investigated. Dislocation related defect was observed in the as-implanted sample. In the DLTS spectra, this dislocation-like defect overlaps with the Z_1/Z_2 deep levels. The dislocation-like defects anneal at 500°C. E_1/E_2 defects were not detected in the as-implanted sample, but they are clearly observed after the 500°C annealing. Deep level at 0.50-0.53eV (possibly E_1 or $RD5$) below the conduction band was observed in the as-implanted sample. E_1/E_2 and the defect at $E_C-0.53$ eV persist after the 1100°C annealing.

ACKNOWLEDGEMENTS

The work described in this paper is supported by the grants from the Research Grant Council of the Hong Kong Special Administrative Region, China (under project Nos. HKU7085/01P, HKU7103/02P, and HKU7034/03P) and the CRCG HKU.

REFERENCES

1. H. Morkoç, S. Strite, G. B. Gao, M. E. Lin, B. Sverdlov, and M. Burns, *J. App. Phys.* **76**, 1362 (1994).
2. G. Pensl and W. J. Choyke, *Physica B* **185**, 264 (1993).
3. T. Dalibor, G. Pensl, H. Matsunami, T. Kimoto, W. J. Choyke, A. Schoener and N. Nordell, *Phys. Stat. Sol. (a)* **162**, 199 (1997).
4. M. O. Aboelfotoh and J. P. Doyle, *Phys. Rev. B* **59**, 10 823 (1999).
5. A. A. Lebedev, A. I. Veinger, D. V. Davydov, V. V. Kozlovski, N. S. Savkina, and A. M. Strel'chuk, *J. Appl. Phys.* **88**, 6265 (2000).
6. Th. Frank, G. Pensl, Song Bai, R. P. Devaty and W. J. Choyke, *Mat. Sci. For.* **338-342**, 753 (2000).
7. C. G. Hemmingsson, N. T. Son, O. Kordina, E. Janzén, and J. L. Lindström, *J. Appl. Phys.* **84**, 704 (1998).
8. M. Gong, S. Fung, C. D. Beling, and Z. You, *J. Appl. Phys.* **85**, 7604 (1999).
9. M. Weidner, T. Frank, G. Pensl, A. Kawasuso, H. Itoh, and R. Krause-Rehberg, *Physica B* **308-310**, 633 (2001).
10. X. D. Chen, S. Fung, C. C. Ling, C. D. Beling, and M. Gong, *J. Appl. Phys.* **94**, 3004 (2003).
11. T. Wosinski, *J. Appl. Phys.* **65**, 1566 (1989).
12. P. Omling, E. R. Weber, L. Montelius, H. Alexander, and J. Michel, *Phys. Rev. B* **32**, 6571 (1985).